Mathematical Formalism to Study Energy Distribution between Base and Walls of Solar Hot Boxes for Mirror Reflected Solar Radiation

Namrata Sengar*‡, Sunita Mahavar**, Prabha Dashora**

*Department of Pure and Applied Physics, University of Kota, Kota, Rajasthan, India

**Department of Physics, University of Rajasthan, Jaipur, India

(namrata@uok.ac.in, smjpr1986@gmail.com, pdashora@yahoo.com)

‡ Corresponding Author; Namrata Sengar, Department of Pure and Applied Physics, University of Kota, Kota, Rajasthan, India, Tel: +91 744 2471038, Mobile: +91 9413007690, namrata@uok.ac.in

Received: 28.11.2018 Accepted:07.02.2019

Abstract- The paper presents a mathematical formalism to study energy absorbed by base plate and walls of the absorber tray due to mirror reflected radiation for a solar hot box. The absorber tray has been considered as composed of five surfaces (base plate and four walls). The study is focused on estimating the reflected solar radiation receiving areas on these five surfaces. The formalism has been developed using solar geometry angles, collector-reflector design parameters, tracking modes with appropriate boundary conditions. The expressions derived for the areas of five surfaces which receive radiation reflected by mirror are presented in form of tables with boundary conditions. The formalism has been studied for various cases such as non-tracked, azimuthally tracked collector with fixed mirror angle and fully tracked modes. The developed formalism can be used in general for any flat plate collector with four walled absorber tray. The results of calculations presented here are for hot box solar cooker with inclined and vertical walls. The study elucidates that reflector is more effective in winters, tracking requirements are less in winters as compared to summers and more effective heating of load can be achieved for collectors with inclined walls. This study may serve as a useful aid in better designing of four walled flat plate collectors such as solar cookers, dryers, distillation stills, water heaters etc.

Keywords- : energy absorption, reflected radiation, flat plate collector, solar cooker, base plate, inclined walls, tracking modes.

1. Introduction

Solar energy is increasingly making its way through both solar PV and thermal technologies [1-6]. The need of the hour is to improve performance of both solar PV and thermal systems. Many of the solar thermal devices such as solar hot box cookers, water heaters, distillation stills and dryers etc. are basically flat plate solar collectors. The performance of the solar collectors can be enhanced by the use of mirror reflectors.

There have been several studies on flat plate collectors related to the estimation of rate of radiation absorbed for different collector orientations, reflector orientations, shading due to single or double reflectors, etc. [7-24]. The earlier studies on collector-reflector system as reported in literature have considered various aspects and parameters but there is no study which focuses on the distribution of the reflected energy between base plate and walls of the absorber tray. In the earlier studies mainly energy absorption has been considered on aperture area only and therefore the distribution of energy absorbed on the base plate and four walls of the absorber tray has not been studied. Solar thermal devices such as hot-box solar cookers, solar stills and dryers etc. based on flat plate collector have absorber tray as an essential component. In these systems the load is placed on the absorber tray which is generally four walled structure with base plate. The energy absorbed by the tray is conducted to the load, thus lesser shading of the base plate and more energy receiving area enhances the thermal performance of the system. The distribution of absorbed energy between base plate and four walls is affected by the wall height and wall inclination of the absorber tray. Nahar and Garg [25] conducted a study for the optimization of the air-gap between absorber plate and cover glazing for minimum convective losses and minimum shading of the absorber base plate due to the vertical side walls. Sengar et.al. [26] developed a mathematical formalism to study energy distribution pattern in solar hot boxes for global solar radiation. The study focused on distribution of energy between the base plate and walls of the absorber tray for global solar radiation. Formalism was developed as a general case for a flat plate tilted collector with off-south orientation. Study related to distribution of mirror reflected energy between base plate and walls of the absorber tray is not to be found in literature therefore the present work focuses on this aspect. The four walled absorber tray has been considered as five surfaces and formalism has been developed to study the energy distribution pattern for mirror reflected solar radiation considering the base plate and walls. Here wall height and wall inclination have also been included. The developed formalism has been studied for flat plate collector for reflected radiation for various cases such as non-tracked, azimuthally tracked collector with fixed mirror angle not adjusted and fully tracked modes.

2. Methodology

The formalism has been developed for a general case of flat plate solar collector which has four walled absorber tray (Fig. 1), thus absorber tray is considered to be composed of five surfaces j=1 to 5. The mathematical expressions with boundary conditions have been developed on the basis of experimental observations of the base plate and wall areas of the tray receiving reflected solar radiation for different months for solar collectors [27, 28].

The basic equations have been taken from the earlier studies mentioned in the literature but the expressions for reflected radiation receiving areas for base plate and walls have been developed separately in the present work. The main steps involved in the present work are

i) Modifying the basic equations related to solar flux and solar geometry angles for five surfaces of the absorber tray

ii) Developing expressions for useful reflected radiation receiving areas with proper boundary conditions for non-tracked case.

iii) The expressions were further modified and developed for different cases such azimuthally tracked with reflector fixed at an angle and fully tracked modes.

iv) Combining above steps and using various parameters related to solar geometry, solar radiation and dimensions of collector-reflector, computer programs were developed for different cases for calculation of energy absorption by base plate and walls of the tray.

The formalism has been developed with continuous systematic study of shadow patterns and radiation receiving surfaces (walls and base plate) of solar hot boxes placed in sun for different months. The mathematical expressions have been derived on the basis of this study of solar hot boxes with vertical and inclined walls.

3. Development of the formalism

For any flat plate collector the general expression for the energy absorbed q due to radiation reflected by the reflector is given by [29,30]

$$q = A_c S \tag{1}$$

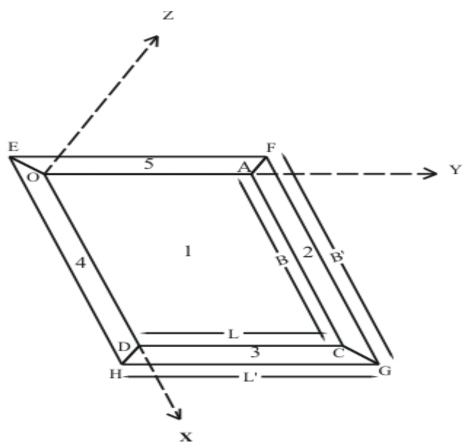

Fig. 1. View of absorber tray with five surfaces.

here A_c is the area of the absorber plate and S is the incident solar flux absorbed by the collector.

For specular reflector

$$S = \rho_r I_{bn} \cos\theta_{ir} \cos\theta_r (\tau_c\alpha)_{br} \tag{2}$$

Here ρ_r is the reflectivity of the reflector, I_{bn} is the beam radiation in the direction of sunrays, θ_{ir} is the angle of incidence of sunrays on the reflector, θ_r is the angle at which the reflected ray strikes the aperture of the collector, $\tau_c\alpha$ is the transmissivity-absortivity product of the glaze for the reflected radiation.

The value of reflectivity and transmissivity of a glaze for solar incidence angle from 0° to 90° can be obtained from the Fresnel laws and equations given below

Reflectivity $$\rho = \frac{1}{2}(\rho_I + \rho_{II}) \tag{3}$$

$$\rho_I = \frac{\sin^2(\theta_r - \theta_i)}{\sin^2(\theta_r + \theta_i)} \tag{4}$$

$$\rho_{II} = \frac{\tan^2(\theta_r - \theta_i)}{\tan^2(\theta_r + \theta_i)} \tag{5}$$

where ρ_I and ρ_{II} are the reflectivities of the two components of polarization.

Similarly transmissivity based on reflection-refraction τ_r is given as

$$\tau_r = \frac{1}{2}\left(\tau_{r_I} + \tau_{r_{II}}\right) \tag{6}$$

where $$\tau_{r_I} = \frac{1-\rho_I}{1+(2M-1)\rho_I} \tag{7}$$

and $$\tau_{r_{II}} = \frac{1-\rho_{II}}{1+(2M-1)\rho_{II}} \tag{8}$$

for M glaze covers.

The transmissivity based on absorption τ_a is given as

$$\tau_a = e^{-Kt/\cos r} \tag{9}$$

where K is extinction coefficient of glaze material, t is the thickness and r is the angle of refraction.

The transmissivity of the transparent cover τ is obtained from product of τ_r and τ_a, i.e.

$$\tau = \tau_r \tau_a \tag{10}$$

Here in this formalism the base plate and walls have been considered so surfaces j= 1 to 5 has been incorporated in the expression. Thus the modified expression becomes

$$q_{ar} = \sum_{j=1}^{5} A_{urj} S_{rj} \tag{11}$$

here j is the index associated with a surface, j = 1represents the absorber base plate and j = 2 to 5 correspond to the four walls of the absorber tray, q_{ar} is the energy absorbed by the absorber tray of the collector due to reflected radiation, A_{urj} is the useful i.e. radiation- receiving area of the j^{th} surface for reflected radiation and S_{rj} is the reflected solar flux absorbed by the j^{th} surface.

For specular reflector the modified expression for solar flux absorbed by j^{th} surface is

$$S_{rj} = \rho_r I_{bn} \cos\theta_{ir} \cos\theta_{rj} \left(\tau_c \alpha_j\right)_{br} \tag{12}$$

Here θ_{rj} is the angle at which the reflected ray strikes the j^{th} surface of the absorber tray and α_j is the absorptivity of the j^{th} absorber surface.

Therefore the expressions for the useful areas A_{urj} are derived as function of angle of incidence of beam radiation on the j^{th} surface (θ_{ij}), zenith angle (θ_z), solar azimuth angle (γ_s), surface azimuth angle of collector (γ), depth of the tray (d), the outward inclination of the walls with respect to the vertical (θ_w), the length (L) and the breadth (B) of the base plate of the absorber tray, the length (L') and the breadth (B') of the aperture of the tray, the slant height or the breadth of the walls (l), tilt angle of the collector (β), the length (L') and width (L_m) of the reflector, the angle that reflector makes with the collector (Ψ) and the tracking conditions.

3.1 Expressions for Useful Absorber Area for Reflected Radiation

Considering a Cartesian coordinate system with origin at one of the corners of the base plate (O), X-axis is along one of the length edge (OD), Y-axis is along one of the breadth edge (OA) of the base plate and Z-axis is normal to the base plate as shown in Fig.1. The sectional view of the absorber tray making an angle β with the horizontal is shown in Fig. 2. It is quite obvious from the figure that the unit vector normal to the absorber base plate ($\mathbf{n_1}$) is

$$\mathbf{n_1} = \mathbf{k} \tag{13}$$

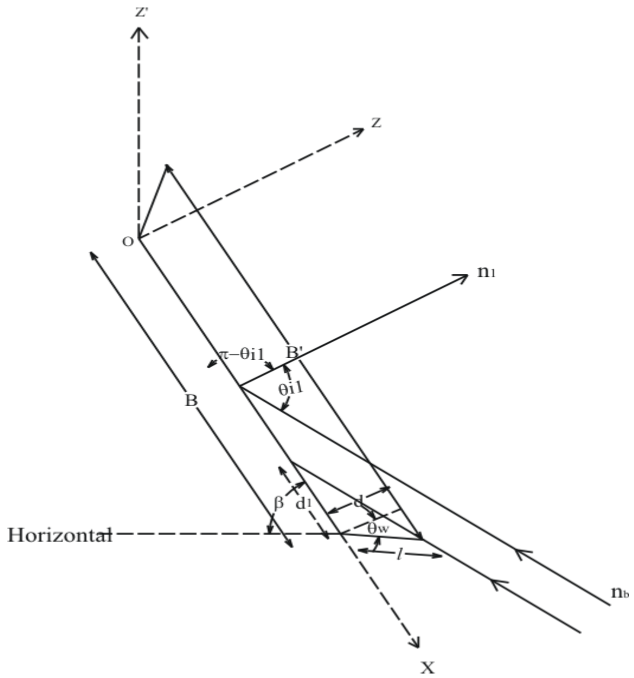

Fig. 2 Sectional view of absorber tray tilted at an angle β.

For obtaining the unit vector along the direction of the beam radiation on a tilted surface, first of all the unit vector is written for a coordinate system (X′Y′Z′) with X′ along South, Y′ along East, Z′ vertical and X′ Y′ plane is horizontal as shown in Fig.3, and then it is transformed from the coordinate system X′Y′Z′ to the coordinate system XYZ.

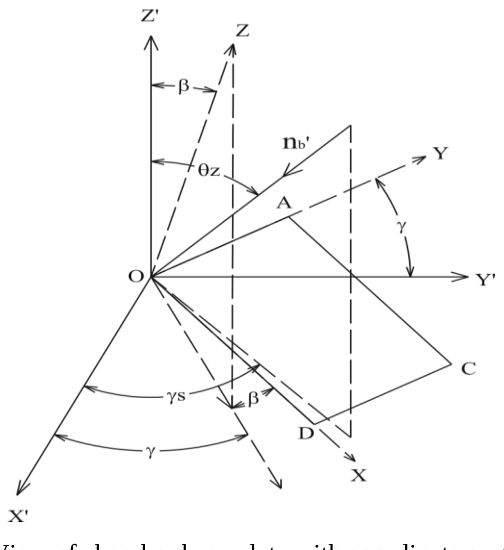

Fig. 3 View of absorber base plate with coordinate systems attached to the collector (XYZ) and ground (X′Y′Z′).

The unit vector along the beam radiation ($\mathbf{n_b'}$) in Cartesian coordinate system X′Y′Z′ is

$$\mathbf{n}_b' = x'\mathbf{i}' + y'\mathbf{j}' + z'\mathbf{k}' \tag{14}$$

here $x' = -\sin\theta_z \cos\gamma_s$, $y' = -\sin\theta_z \sin\gamma_s$, and $z' = -\cos\theta_z$.

Accordingly, $\mathbf{n}'_{\mathbf{b}} = -\sin\theta_z \cos\gamma_s \mathbf{i}' - \sin\theta_z \sin\gamma_s \mathbf{j}' - \cos\theta_z \mathbf{k}'$ (15)

Let $\mathbf{n_b}$ is the unit vector along the beam radiation in the tilted coordinate system (XYZ) of the tray as shown in Fig.2 then

$$\mathbf{n_b} = x\mathbf{i} + y\mathbf{j} + z\mathbf{k} \tag{16}$$

where the values of *x*, *y* and *z* can be found in terms of *x*′, *y*′ and *z*′ through the following transformation equation.

$$\begin{pmatrix} x \\ y \\ z \end{pmatrix} = \begin{pmatrix} \cos\beta\cos\gamma & \cos\beta\sin\gamma & -\sin\beta \\ -\sin\gamma & \cos\gamma & 0 \\ \sin\beta\cos\gamma & \sin\beta\sin\gamma & \cos\beta \end{pmatrix} \begin{pmatrix} x' \\ y' \\ z' \end{pmatrix} \tag{17}$$

$$\begin{aligned} x &= \cos\beta\cos\gamma\, \mathrm{x}' + \cos\beta\sin\gamma\, \mathrm{y}' - \sin\beta\, \mathrm{z}' \\ &= -\sin\theta_z \cos\beta\cos(\gamma - \gamma_s) + \sin\beta\cos\theta_z \end{aligned} \tag{18}$$

$$\begin{aligned} y &= -\sin\gamma\, \mathrm{x}' + \cos\gamma\, \mathrm{y}' \\ &= -\sin\theta_z \sin\gamma_s \cos\gamma + \sin\theta_z \cos\gamma_s \sin\gamma \\ &= \sin\theta_z \sin(\gamma - \gamma_s) \end{aligned} \tag{19}$$

$$\begin{aligned} z &= \cos\gamma\sin\beta\, \mathrm{x}' + \sin\gamma\sin\beta\, \mathrm{y}' + \cos\beta\, \mathrm{z}' \\ &= -\sin\theta_z \sin\beta \cos(\gamma - \gamma_s) - \cos\beta\cos\theta_z \end{aligned} \tag{20}$$

and hence

$$\begin{aligned} \mathbf{n_b} = &\left[-\sin\theta_z \cos\beta\cos(\gamma - \gamma_s) + \sin\beta\cos\theta_z\right]\mathbf{i} \\ &+ \sin\theta_z \sin(\gamma - \gamma_s)\,\mathbf{j} \\ &- \left[\sin\theta_z \sin\beta\cos(\gamma - \gamma_s) + \cos\beta\cos\theta_z\right]\mathbf{k} \end{aligned} \tag{21}$$

The following are the expressions for the normal to the four walls of the absorber tray

$$\begin{aligned} \mathbf{n_2} &= -\cos\theta_w \mathbf{j} + \sin\theta_w \mathbf{k}, \\ \mathbf{n_3} &= -\cos\theta_w \mathbf{i} + \sin\theta_w \mathbf{k}, \\ \mathbf{n_4} &= \cos\theta_w \mathbf{j} + \sin\theta_w \mathbf{k}, \\ \mathbf{n_5} &= \cos\theta_w \mathbf{i} + \sin\theta_w \mathbf{k} \end{aligned} \tag{22}$$

and the angle of incidence of the direct radiation on the j^{th} surface (θ_{ij}) is

$$\cos\theta_{ij} = -(\mathbf{n_j}).(\mathbf{n_b}) \quad \text{here } j = 1 \text{to } 5 \tag{23}$$

Let the angle of incidence of the sunrays on the base plate be θ_{i1} as shown in Fig. 2 and γ is the surface azimuth angle of the collector then

$$\begin{aligned} \cos(\pi - \theta_{i1}) &= \mathbf{n_1}.\mathbf{n_b} \\ \cos\theta_{i1} &= \cos\theta_z \cos\beta + \sin\theta_z \sin\beta\cos(\gamma - \gamma_s) \end{aligned} \tag{24}$$

$$\begin{aligned} \cos\theta_{i2} = &\sin\theta_z \cos\theta_w \sin(\gamma - \gamma_s) + \sin\theta_w \sin\beta\sin\theta_z \cos(\gamma - \gamma_s) \\ &+ \sin\theta_w \cos\beta\cos\theta_z \end{aligned} \tag{25}$$

$$\begin{aligned} \cos\theta_{i3} = &-\sin\theta_z \cos(\gamma - \gamma_s)\cos(\theta_w + \beta) \\ &+ \cos\theta_z \sin(\beta + \theta_w) \end{aligned} \tag{26}$$

$$\begin{aligned} \cos\theta_{i4} = &-\cos\theta_w \sin\theta_z \sin(\gamma - \gamma_s) \\ &+ \sin\theta_w \sin\theta_z \sin\beta\cos(\gamma - \gamma_s) \\ &+ \sin\theta_w \cos\beta\cos\theta_z \end{aligned} \tag{27}$$

$$\begin{aligned} \cos\theta_{i5} = &\sin\theta_z \cos(\gamma - \gamma_s)\cos(\theta_w - \beta) \\ &+ \cos\theta_z \sin(\theta_w - \beta) \end{aligned} \tag{28}$$

The surface azimuth angles of the walls in terms of γ are as follows

$$\gamma_2 = 90° + \gamma, \gamma_3 = \gamma, \gamma_4 = 90° - \gamma \text{ and } \gamma_5 = 180° - \gamma \tag{29}$$

Let the mirror reflector be attached to the top northern edge of the collector and is adjusted such that it makes an angle *Ψ* with the aperture surface as shown in Fig. 4. The reflector has the common edge *L* with the collector. The width of the reflector is L_m. It has been assumed that the reflection is specular. The expressions for the useful areas for reflected radiation falling on the absorber base plate as well as on the walls may be deduced as explained below.

From the Fig. 4 it can be seen that the unit vector normal to the reflector surface, $\mathbf{n_r}$, is

$$\mathbf{n_r} = \sin\psi\, \mathbf{i} - \cos\psi\, \mathbf{k} \tag{30}$$

The solar incident angle on the reflector (θ_{ir}) may be obtained as

$$\begin{aligned} \cos\theta_{i\mathrm{r}} &= -\mathbf{n_b}.\mathbf{n_r} \\ &= \sin\theta_z \cos(\gamma - \gamma_s)\sin(\psi - \beta) - \cos\theta_z \cos(\psi - \beta) \end{aligned} \tag{31}$$

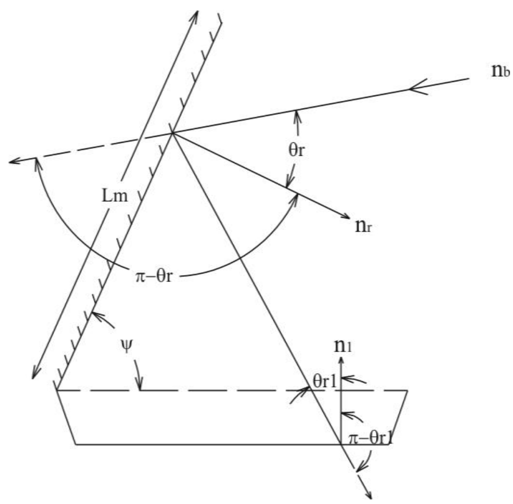

Fig. 4. Sectional view of collector with reflector adjusted at an angle ψ with the glaze.

According to the laws of reflection in vector algebra, the unit vector along the reflected ray that strikes the collector $\mathbf{n_{r1}}$ [14]

$$\begin{aligned} \mathbf{n_{r1}} &= \mathbf{n_b} - 2[(-\mathbf{n_r}).(\mathbf{n_b})](-\mathbf{n_r}) \\ &= \mathbf{n_b} + 2[(-\mathbf{n_r}).\mathbf{n_b}]\mathbf{n_r} \end{aligned} \tag{32}$$

The components of $\mathbf{n_{r1}}$ along the X, Y and Z-axes are

$$x_1 = \cos\theta_z \sin(\beta - 2\psi) - \sin\theta_z \cos(\beta - 2\psi)\cos(\gamma - \gamma_s) \quad (33)$$

$$y_1 = \sin\theta_z \sin(\gamma - \gamma_s) \quad (34)$$

and

$$z_1 = \cos\theta_z \cos(\beta - 2\psi) + \sin\theta_z \sin(\beta - 2\psi)\cos(\gamma - \gamma_s) \quad (35)$$

The angle θ_{rj} at which the reflected ray strikes the jth surface of the absorber tray may be obtained as

$$\cos\theta_{rj} = -n_{r1}.n_j \quad (36)$$

$$\cos\theta_{r1} = -\mathbf{n_{r1}}.\mathbf{n_1} = -\cos\theta_z \cos(\beta - 2\psi) - \sin\theta_z \sin(\beta - 2\psi)\cos(\gamma - \gamma_s) \quad (37)$$

$$\cos\theta_{r2} = \cos\theta_w \sin\theta_z \sin(\gamma - \gamma_s) - \sin\theta_w \left[\cos\theta_z \cos(\beta - 2\psi) + \cos(\gamma - \gamma_s)\sin\theta_z \sin(\beta - 2\psi)\right] \quad (38)$$

$$\cos\theta_{r3} = \cos\theta_z \sin(\beta - 2\psi - \theta_w) - \cos(\gamma - \gamma_s)\sin\theta_z \cos(\beta - 2\psi - \theta_w) \quad (39)$$

$$\cos\theta_{r4} = -\cos\theta_w \sin\theta_z \sin(\gamma - \gamma_s) - \sin\theta_w\left[\cos\theta_z \cos(\beta - 2\psi) + \cos(\gamma - \gamma_s)\sin\theta_z \sin(\beta - 2\psi)\right] \quad (40)$$

$$\cos\theta_{r5} = -\cos\theta_z \sin(\beta - 2\psi + \theta_w) + \cos(\gamma - \gamma_s)\sin\theta_z \cos(\beta - 2\psi + \theta_w) \quad (41)$$

These angles are used in estimating the absorption of solar radiation on different surfaces of the solar hot box absorber tray i.e. walls and base plate using eq. 12.

3.1.1 Useful Base Plate Area for Reflected Radiation

If the mirror orientation is kept fixed then the length of reflected light (L_r) can lie within the base plate or overextend it depending on the Ψ, θ_{i1}, γ_s *and* γ.

From the Fig.5 it can be seen that 'b_s', the section of the breadth of the base plate where the reflected light does not reach due to the back wall height and the mirror angle adjustment, is given by

$$b_s = d\ \tan\theta_{r1} \cos|\gamma - \gamma_s| - \mathrm{d}\ \tan\theta_w \quad (42)$$

The value of b_s can be positive or negative at any instant as can be seen from the Fig. 5 and 6.

The breadth of base plate 'b' which is not in shade due to the back wall is

$$b = B - b_s \text{ if } \tan\theta_{r1} \cos|\gamma - \gamma_s| - \tan\theta_w > 0 \quad (43)$$

$$\text{and } b = B \text{ if } \tan\theta_{r1} \cos|\gamma - \gamma_s| - \tan\theta_w \le 0 \quad (44)$$

The length of reflected light (L_r) on the plane containing base plate of the tray is given by

$$L_r = L_m \cos\psi + \mathrm{L_m}\ \sin\psi\ \tan\theta_{r1} \text{ if } \tan\theta_{r1} \cos|\gamma - \gamma_s| - \tan\theta_w > 0 \quad (45)$$

$$L_r = L_m \cos\psi + \mathrm{L_m}\ \sin\psi\ \tan\theta_{r1} + \mathrm{d}\ \tan\theta_{r1} - \mathrm{d}\ \tan\theta_w \text{ if } \tan\theta_{r1} \cos|\gamma - \gamma_s| - \tan\theta_w \le 0 \quad (46)$$

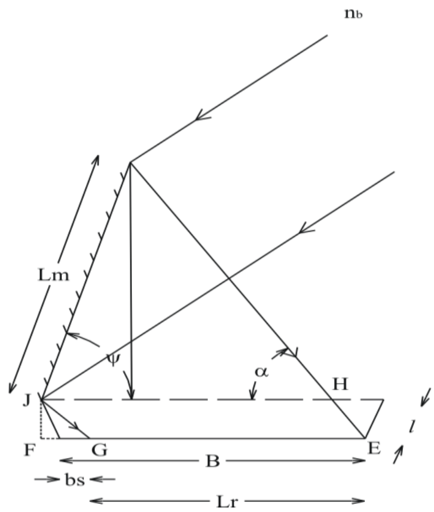

Fig.5. Collector with reflector adjusted at an angle ψ such that b_s is positive.

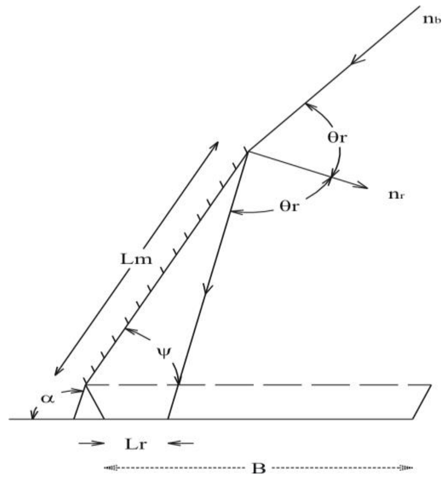

Fig. 6. Collector with reflector adjusted at an angle ψ such that b_s is negative.

The section of the length of the base plate where the reflected light does not reach due to the side wall height and the mirror angle adjustment has been expressed as L_s, which is given by

$$L_s = d\ \tan\theta_{r1} \sin|\gamma - \gamma_s| - \mathrm{d}\ \tan\theta_w \quad (47)$$

The area of the base plate that receives reflected radiation has been expressed as A_{ur1} for the various conditions of L_r, b, L_s, γ_s and γ. For $|\gamma - \gamma_s| > 90^o$ and $\theta_{ir} > 90^o$ the sun would be at the back of mirror and in that case instead of reflected radiation, shadow of the mirror would fall on the absorber tray. The various expressions of A_{ur1} for the different orientations of collector and mirror and for the changing solar angles are presented in Table 1 and Fig. 7.

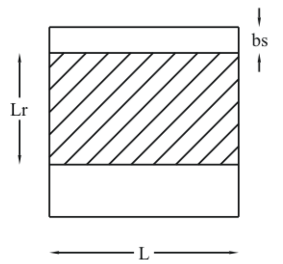

Fig. 7(i). $L_r < b$ and $|\gamma - \gamma_S|$ =0.

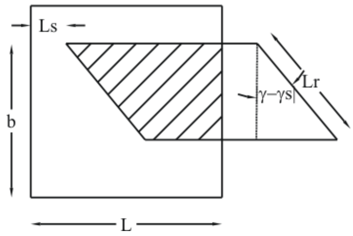

Fig. 7(ii). $L_r\, cos|\gamma - \gamma_S| < b$ and $b\, tan|\gamma - \gamma_S| + L_s < L$.

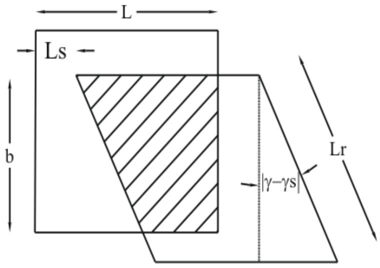

Fig. 7(iii). $L_r\, cos|\gamma - \gamma_S| \geq b$ and $b\, tan|\gamma - \gamma_S| + L_s < L$.

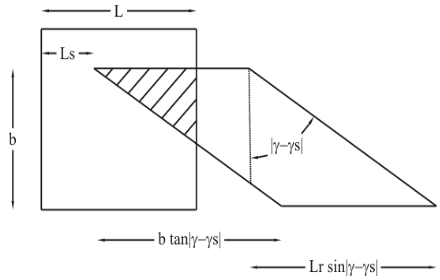

Fig. 7(iv). $L_r\, cos|\gamma - \gamma_S| \geq b$ and $b\, tan|\gamma - \gamma_S| + L_s \geq L$.

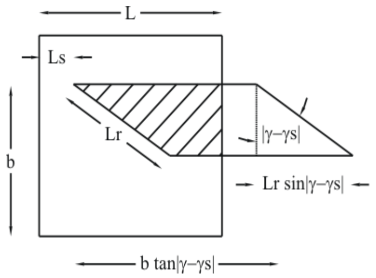

Fig. 7(v). $L_r\, cos|\gamma - \gamma_S| < b$, $b\, tan|\gamma - \gamma_S| + L_s > L$ and $L_r\, sin|\gamma - \gamma_S| <$ L.

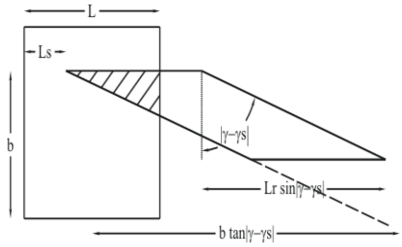

Fig. 7(vi). $L_r\, cos|\gamma - \gamma_S| < b$, $b\, tan|\gamma - \gamma_S| + L_s > L$ and $L_r\, sin\, |\gamma - \gamma_S| \geq L$.

Fig. 7. Hatched portion shows the radiation receiving absorber base plate area A_{ur1} for conditions mentioned below each figure [7(i) to 7(vi), Table 1].

Table 1: Absorber base plate area that receives reflected radiation when collector is non-tracked oriented off-south.

Conditions	Area A_{r1}	Figure
$L_r < b, \lvert\gamma - \gamma_s\rvert = 0$	$L\,.\,L_r$	Fig. 7(i)
$L_r \geq b, \lvert\gamma - \gamma_s\rvert = 0$	$L\,.\,b$	-
$L_r \cos\lvert\gamma - \gamma_s\rvert < b$ $b \tan\lvert\gamma - \gamma_s\rvert + L_s < L$	$\frac{1}{2}\left(2L - 2L_s - L_r \sin\lvert\gamma - \gamma_s\rvert\right) L_r \cos\lvert\gamma - \gamma_s\rvert$	Fig. 7(ii)
$L_r \cos\lvert\gamma - \gamma_s\rvert \geq b$ $b \tan\lvert\gamma - \gamma_s\rvert + L_s < L$	$\frac{1}{2}\left(2L - 2L_s - b \tan\lvert\gamma - \gamma_s\rvert\right) b$	Fig. 7(iii)
$L_r \cos\lvert\gamma - \gamma_s\rvert \geq b$ $b \tan\lvert\gamma - \gamma_s\rvert + L_s \geq L$	$\frac{1}{2}(L - L_s)^2 \cot\lvert\gamma - \gamma_s\rvert$	Fig. 7(iv)
$L_r \cos\lvert\gamma - \gamma_s\rvert < b$ $b \tan\lvert\gamma - \gamma_s\rvert + L_s > L$ $L_r \sin\lvert\gamma - \gamma_s\rvert < L$	$\frac{1}{2}\left(2L - 2L_s - L_r \sin\lvert\gamma - \gamma_s\rvert\right) L_r \cos\lvert\gamma - \gamma_s\rvert$	Fig. 7(v)
$L_r \cos\lvert\gamma - \gamma_s\rvert < b$ $b \tan\lvert\gamma - \gamma_s\rvert + L_s > L$ $L_r \sin\lvert\gamma - \gamma_s\rvert \geq L$	$\frac{1}{2}(L - L_s)^2 \cot\lvert\gamma - \gamma_s\rvert$	Fig. 7(vi)

3.1.2 Useful Wall Area for Reflected Radiation

The expressions for the useful wall area have been deduced here considering the boundary conditions on $L_r \cos|\gamma - \gamma_s|$. When $|\gamma - \gamma_s| \neq 0$ and $\theta_{ir} < 90^o$ then one or two walls may receive reflected radiation at an instant depending on the boundary conditions.

When $L_r \cos|\gamma - \gamma_s| <$ b then either the wall surface '2' or wall surface'4' would receive reflected radiation (sidewall). If $b < L_r \cos|\gamma - \gamma_s| < b+l$ or $b+l < L_r \cos|\gamma - \gamma_s|$ then wall surface '3' (front wall opposite to reflector) and one of the walls '2 or 4' would receive reflected radiation at an instant. Wall surface '2' would receive reflected light if the projection of the incident sunrays on the horizontal plane lies to the west of the projection of the normal of the base plate.

Similarly wall '4' would receive reflected light if the projection of the incident sunrays on the horizontal plane lies to the east of the projection of the normal of the base plate. The useful wall area of the absorber that receives the reflected radiation at any instant is given by the following expressions presented in the Fig. 8 and Table 3 for the different conditions on $L_r \cos|\gamma - \gamma_s|$.

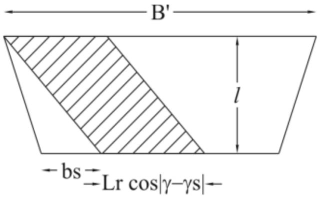

Fig. 8(i) $L_r \cos|\gamma - \gamma_S| \leq b$, $b \tan|\gamma - \gamma_S| + L_s > L$, $L_r \sin|\gamma - \gamma_S| < L$. (Side wall)

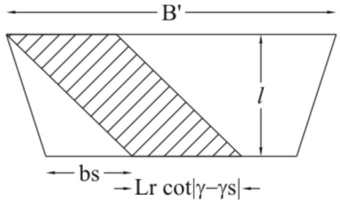

Fig. 8(ii) $L_r \cos|\gamma - \gamma_S| \leq b$, $b \tan|\gamma - \gamma_S| + L_s > L$, $L_r \sin|\gamma - \gamma_S| > L$. (Side wall)

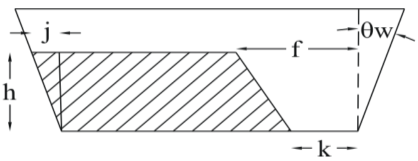

Fig. 8(iii) $b < L_r \cos|\gamma - \gamma_S| < b + l$

$b \tan|\gamma - \gamma_S| + L_s \leq L$. (Front wall)

h = $L_r \cos|\gamma - \gamma_S| - b$, k = $b \tan|\gamma - \gamma_S| + L_s$

j = h $\tan\theta_w$ and f = $L_r \sin|\gamma - \gamma_S| + L_s$.

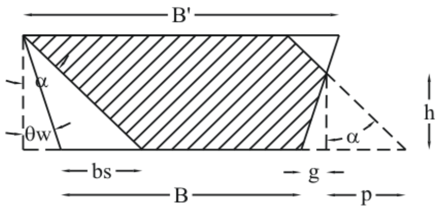

Fig. 8(iv) $b < L_r \cos|\gamma - \gamma_S| < b + l$,

and $b \tan|\gamma - \gamma_S| + L_s \leq L$. (Side wall)

$\tan\alpha = \tan\theta_w + b_s / l$, p = h $\tan\alpha$
and g = h $\tan\theta_w$.

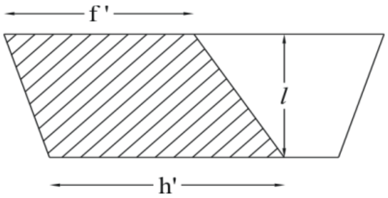

Fig. 8(v) $b + l < L_r \cos|\gamma - \gamma_S|$ and $b \tan|\gamma - \gamma_S| + L_s \leq L$. (Front wall)

$f' = L' - (b+l) \tan|\gamma - \gamma_S| - L_s$ and $h' = L - b \tan|\gamma - \gamma_S| - L_s$

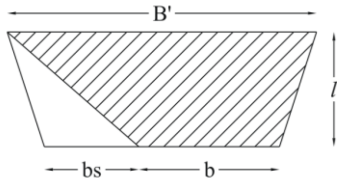

Fig. 8(vi) $b + l < L_r \cos|\gamma - \gamma_S|$ and $b \tan|\gamma - \gamma_S| + L_s \leq L$. (Side wall)

Fig. 8. Absorber wall (front/side wall) area receiving reflected radiation shown as hatched portion for the conditions mentioned below each figure and expressions are presented in Table 2.

Table 2: Absorber wall area that receives reflected radiation when collector is non-tracked oriented off-south.

Conditions		Area	Figure
$\lvert\gamma - \gamma_s\rvert \neq 0$ *and*	$L_r \cos\lvert\gamma - \gamma_s\rvert \leq b$ *and* $L_r \sin\lvert\gamma - \gamma_s\rvert < L$	$A_{rw2/4} = L_r \cos\lvert\gamma - \gamma_s\rvert l$	Fig. 7(v), Fig.8(i)

	$L_r \cos\lvert\gamma - \gamma_s\rvert \le b$ *and* $L_r \sin\lvert\gamma - \gamma_s\rvert > L$	$A_{rw2/4} = (L - L_s)\cot\lvert\gamma - \gamma_s\rvert\, l$	Fig. 7(vi), Fig.8(ii)
	$L_r \cos\lvert\gamma - \gamma_s\rvert > b$	$A_{rw2/4} = (L - L_s)\cot\lvert\gamma - \gamma_s\rvert\, l$	Fig. 7(vi), Fig.8(ii)
$\lvert\gamma - \gamma_s\rvert \ne 0$ *and* $b\tan\lvert\gamma - \gamma_s\rvert + L_s \le L$	$L_r \cos\lvert\gamma - \gamma_s\rvert < b$	$A_{rw2/4} = L_r \cos\lvert\gamma - \gamma_s\rvert\, l$	Fig. 7(v), Fig.8(i)
	$b < L_r \cos\lvert\gamma - \gamma_s\rvert < b + l$	$A_{rw3} = \frac{1}{2}\left(L_r \cos\lvert\gamma - \gamma_s\rvert - b\right)\times \left[2L - b\tan\lvert\gamma - \gamma_s\rvert - L_r \sin\lvert\gamma - \gamma_s\rvert + \left(L_r \cos\lvert\gamma - \gamma_s\rvert - b\right)\tan\theta_w\right]$ $A_{rw2/4} = \left(L_r \cos\lvert\gamma - \gamma_s\rvert - b\right)\times \left(2l - L_r \cos\lvert\gamma - \gamma_s\rvert + b\right)\left(\tan\theta_w + \frac{b_s}{2l}\right) + bl$	Fig. 8(iii) Fig. 8(iv)
	$b + l < L_r \cos\lvert\gamma - \gamma_s\rvert$	$A_{rw3} = \frac{1}{2}\left[L - b\tan\lvert\gamma - \gamma_s\rvert + L' - (b + l)\tan\lvert\gamma - \gamma_s\rvert\right] l$ $A_{rw2/4} = \frac{1}{2}(b + B')\, l$	Fig. 8(v) Fig. 8(vi)
$\lvert\gamma - \gamma_s\rvert = 0$	$L_r \le b$	$A_{rw2\,\mathrm{and}\,4} = L_r\, l$	
	$b < L_r < b + l$	$A_{rw3} = \frac{1}{2}(L_r - b)\times\left[2L + (L_r - b)\tan\theta_w\right]$ $A_{rw2\,\mathrm{and}\,4} = bl + (L_r - b)(2l - L_r + b)\left(\tan\theta_w + \frac{b_s}{2l}\right)$	
	$b + l < L_r$	$A_{rw3} = \frac{1}{2}\left[L + L'\right] l$ and $A_{rw2\,\mathrm{and}\,4} = \frac{1}{2}(b + B')\, l$	

3.1.3 Total Useful Absorber Area for Reflected Radiation

The total useful absorber area A_{ur} at any instant for the reflected radiation is given by the summation of the useful areas for reflected radiation of the five surfaces corresponding to j=1 to 5. Thus

$$A_{ur} = \sum_{j=1}^{5} A_{urj} \tag{48}$$

3.2 Angular Adjustment of Reflector for Maximum Reception of Reflected Light on Absorber Base Plate

An equation has been developed for angular adjustment of reflector for azimuthally tracked condition, when the sunrays do not over extend the base. The condition has been considered because the heat transfer does not take place directly between the load and the walls, though indirectly by conduction some heat may be coupled to the load. By adjusting the limiting rays on base plate boundary and not allowing extending on the front wall the angle of incidence becomes less for base plate and the shadow area towards the back wall is less. Both these factors give positive contribution towards increased absorption of radiation on the base plate area.

The breadth of the base plate

$$B = b_s + GE \tag{49}$$

$$GE = JH = L_m \cos\psi + L_m \sin\psi \cot\alpha \tag{50}$$

$$\text{and } b_s = d\cot\alpha - d\tan\theta_w \tag{51}$$

here α is the angle at which reflected ray strikes the horizontal glaze and base plate.

$$\therefore B = d\cot\alpha - d\tan\theta_w + L_m \cos\psi + L_m \sin\psi \cot\alpha \tag{52}$$

$$\because \alpha = 270 - \theta_z - 2\psi \tag{53}$$

$$B = L_m \cos\psi + L_m(\sin\psi + d)\tan(\theta_z + 2\psi) - d\tan\theta_w \tag{54}$$

Above equation can be solved numerically to render the values of ψ for known L_m, B, d, θ_z and θ_w. Here L_m, B, d and θ_w are the design parameters of the system and θ_z, the zenith angle depends on the solar geometry.

3.3 Expressions for Useful Absorber Area for Some Special Cases

3.3.1 Non Tracked South Facing Collector

Generally south facing solar systems are preferred in non-tracked mode for places in northern hemisphere for maximum interception of solar radiation year round. For this case the expressions for useful absorber areas are same as mentioned in Table 1 and 2, the only difference being that

$|\gamma - \gamma_s|$ is replaced by $|\gamma_s|$ as the surface azimuth angle γ for the collector is zero.

3.3.2 Azimuthally Tracked Collector with Fixed Mirror Inclination

If a collector is tracked azimuthally i.e. the collector follows the sun's motion in east-west direction then mathematically $|\gamma - \gamma_s|$ =0. This particular case is of physical significance while considering a collector operating with a single axis tracking system (azimuthal tracking).

When the collector is tracked azimuthally but the angular adjustment of the mirror reflector is not done according to the altitude angle of the sun i.e. the angle that reflector makes with the collector plane is kept fixed, the area of the base plate that receives reflected radiation is given by

$$A_{ur1} = L \,.\, L_r \quad \text{if } L_r < b \qquad \text{Fig.7(i)} \tag{55}$$

$$A_{ur1} = L \,.\, b \quad \text{if } L_r \geq b \tag{56}$$

The relations for the useful wall area corresponding to reflected radiation for a collector, which is tracked azimuthally but the mirror adjustment is not done have been presented in Table 3.

Table 3: Absorber wall area that receives reflected radiation when collector is tracked azimuthally with fixed mirror inclination

Conditions	Area
$L_r \leq b$	$A_{rw2\,\text{and}\,4} = L_r\, l$
$b < \mathrm{L_r} < b + l$	$A_{rw3} = \frac{1}{2}(L_r - b) \times [2L + (L_r - b)\tan\theta_w]$
	$\mathrm{A_{rw2\,and\,4}} = bl + (L_r - b)\left(\tan\theta_w + \frac{b_s}{2l}\right)(2l - L_r + b)$
$b + l < L_r$	$A_{rw3} = \frac{1}{2}[L + L']\, l$
	$\mathrm{A_{rw2\,and\,4}} = \frac{1}{2}(b + B')l$

3.3.3 Fully tracked mode

The case when collectors are tracked azimuthally and mirror is also adjusted is the optimal case where maximum energy gain can be achieved in case of solar cookers and hence considered as fully tracked mode. This is helpful while comparing the energy gain in different tracking modes. The area of the base plate that receives reflected radiation in this case would be

$$A_{ur1} = L \,.\, b \tag{57}$$

Here it is assumed that the angular adjustment is done in such a way that the rays reflected from the topmost edge of the reflector reach the front edge of the base plate as presented in section 3.2. Hence in this case the front wall (surface 3) would not receive reflected radiation but the two sidewalls would have the following radiation receiving area

$$A_{ur2\,\text{and}\,4} = L_r\, l \tag{58}$$

here L_r is equal to b.

3.3.4 Collector having Absorber Tray with Vertical Walls

Quite often due to the fabrication simplicity or cost benefits the flat plate solar collectors, which have absorber tray with vertical walls are used in several solar thermal appliances such as solar water heaters, dryers and distillation stills. Therefore for the estimation of the useful absorber area for such a collector θ_w = 0 should be used in the expressions presented in tables 1-3.

4. Computations

The developed formalism has been used to study the pattern of energy absorbed by the base plate and walls of the absorber tray for reflected radiation. The computations and results presented here are for commercial hot box solar cooker CSC (Fig. 9).

Fig. 9. The common commercial fiber body hot box solar cooker (CSC).

Further the computations have been done for energy received by the aperture and it has been verified that the sum of the energy absorbed by the base plate and walls is equal to the energy absorbed by the aperture area. A computer program was prepared in Qbasic on the basis of developed formalism taking into account the parameters viz. θ_{ij}, γ_s, γ, d, θ_w, L, B, L', B', l, β and incorporating the various conditions and expressions presented in section 3. The details of the parameters used in the computations are given in Table 4.

The extinction coefficient and refractive index of glass sheet have been taken as 15 m^{-1} and 1.52 respectively. The value of τ_c and the tilt factors have been calculated [29]. The values of I_b and I_d have been obtained through ASHRAE method, where the values of A, B and C used in the calculations are the revised values given by Iqbal [30]. During the calculations the average value of absorptance has been taken for a day depending on the variation of the incidence angle. On Dec-21 (δ=-23.45°) the angles vary from 50 to 77° and the absorptance would vary from 0.91 to 0.81, therefore average value of 0.86 for absorptance has been used in the program. Similarly for δ = 0° and δ = 23.45° the average values of absorptance are taken as 0.93 and 0.94 respectively [31]. The reflectivity of the mirror has been taken as 0.80. The calculations have been done for the tracking modes (i) non-tracked south facing mode when reflector is adjusted for maximum reception of solar radiation on the base plate during solar noon (mode A) (ii) azimuthally tracked mode when reflector is adjusted for maximum reception of solar radiation on the base plate during solar noon (mode B) (iii) fully tracked mode where azimuthal tracking is considered along with the continuous optimum adjustment of the reflector (mode C). The reflector angle (ψ) for maximum reception of reflected radiation on the base plate for various declination values calculated using eq. 54 for CSC with wall inclinations 0^o and 20^o has been presented in table 5.

Table 4: Parameters used in computations.

S. No.	Parameters	Details			
1.	CSC (20^o) dimensions	Base plate-0.16 sq.m. (0.4 m × 0.4 m.)	Aperture-0.21 sq.m. (0.46 m × 0.46 m.)	Wall height-0.084 m.	Wall inclination-20^o
2.	CSC (0^o) dimensions	Base plate-0.16 sq.m. (0.4 m × 0.4 m.)	Aperture 0.16 sq.m. (0.4 m × 0.4 m.)	Wall height-0.084 m.	Wall inclination-0^o
3.	Glass sheet	Extinction coefficient-15 m^{-1}	Refractive index-1.52	Number of sheets -2	Thickness of each-4mm
4.	Absorptance	0.86 for δ = -23.45^o	0.93 for δ = 0^o	0.94 for δ = $+23.45^o$	
5.	Location and time	Jaipur (India)	Latitude-26.55°N	Longitude-75.52°E	Solar time-8 a.m. to 4 p.m.
6.	Tracking modes	Mode A Non-tracked	Mode B Azimuthally tracked with fixed mirror inclination		Mode C Fully tracked

Table 5: Reflector angle (ψ) for maximum reception of reflected radiation on the base plate for various declination values.

Solar Time (hr)	CSC (0^o)			CSC (20^o)		
	ψ (δ = -23.45°) in degrees	ψ (δ = 0°) in degrees	ψ (δ = 23.45°) in degrees	ψ (δ = -23.45°) in degrees	ψ (δ = 0°) in degrees	ψ (δ = 23.45°) in degrees
8:00	65.5	74.5	80.5	64	73	79.5
9:00	72.5	82.5	89	71	81.5	88.5
10:00	78	90	98	77	89.5	97.5
11:00	81.5	96	107	81	95.5	106.5
12:00	83	98.5	114	82	98	114
13:00	81.5	96	107	81	95.5	106.5
14:00	78	90	98	77	89.5	97.5
15:00	72.5	82.5	89	71	81.5	88.5
16:00	65.5	74.5	80.5	64	73	79.5

5. Results and discussions

Fig. 10 shows the variation in energy absorbed by the base plate and walls of the collector with θ_w=20^o for reflected radiation with solar time on three different days of a year. Here the collector is considered to be kept in non-tracked mode when reflector is south facing and is inclined at an angle ψ with the collector such that maximum solar radiation is received at the base plate at local solar noon. It is quite interesting to observe that the maximum reflected energy is absorbed on Dec-21 followed by Mar-21 and Jun-21. The energy absorbed at the solar noon due to the reflected radiation on Dec-21 is 130% more than Jun-21 and 31% more as on Mar-21.Thus the loss in energy absorbed due to less global radiation in winters can be compensated to some extent with the use of reflector. Curve for Jun-21 reveals that if reflector angle is kept fixed for maximum reception at local solar noon then the enhancement in energy absorbed due to reflected radiation is for very short duration 11:30 to 12:30 and that too is only 10-12% of the solar radiation absorbed. Therefore in summers the role of reflector fixed in one position is almost negligible and the system can be used without it.

The energy absorption by the base plate and walls of the collector with vertical walls (θ_w=0^o) for reflected radiation has been shown in fig. 11 for three different declinations. On comparing fig. 10 and 11, it can be seen that radiation absorbed by the base plate in December is 18% more for the systems with inclined walls though the energy absorbed by the walls is almost equal. As expected the energy absorption by the base plate and walls is 10-40% higher in March and June for the system with inclined walls.

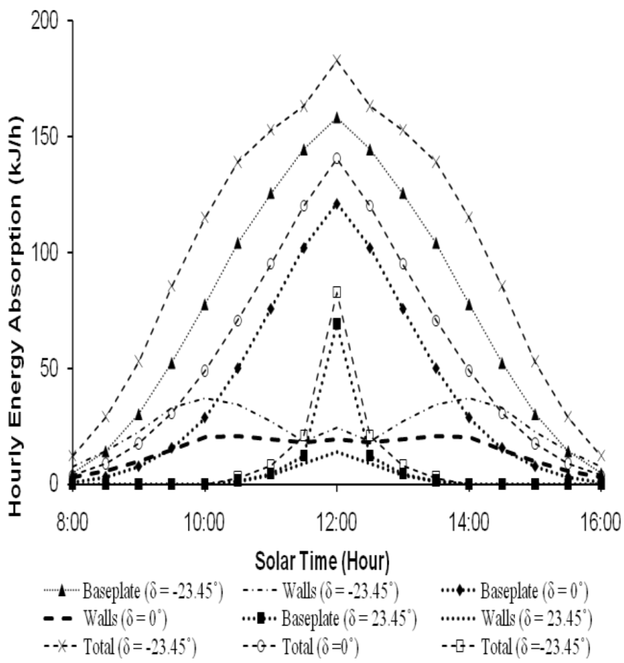

Fig. 10. Variation in hourly energy absorbed by the base plate and walls of the solar collector CSC (20^o) for reflected radiation for three different declinations (δ).

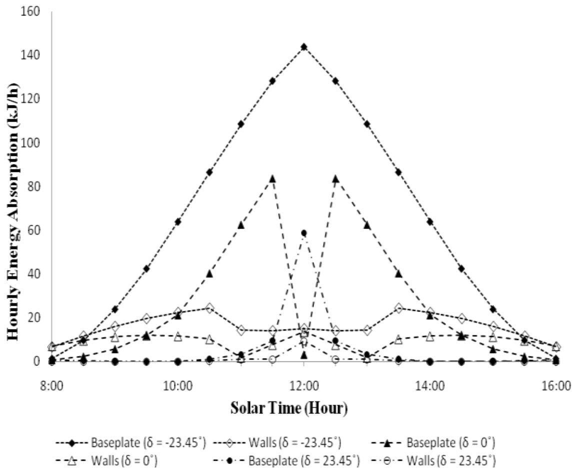

Fig. 11. Variation in hourly energy absorbed by the base plate and walls of the solar collector CSC (0^o) for reflected radiation for three different declinations (δ).

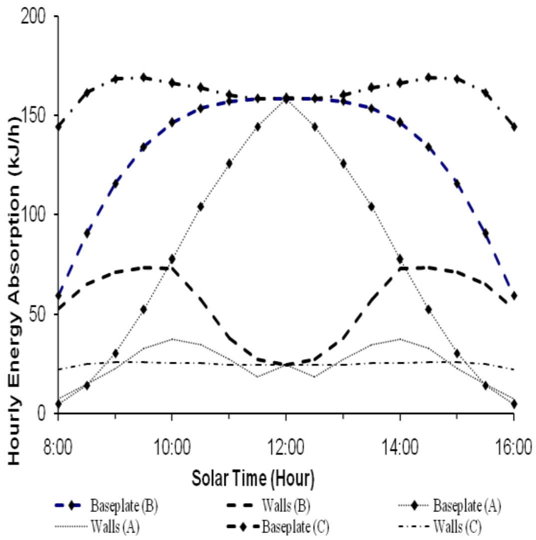

Fig. 12. Variation in hourly energy absorbed by the base plate and walls of the solar collector for different tracking modes A, B and C for reflected radiation on Dec-21 (δ = -23.45^o).

The effect of various tracking modes on the energy absorbed by the CSC (wall inclination 20^o) due to the reflected radiation for three different days (Dec-21, Mar-21 and Jun-21) of a year has been presented in the form of graphs in Fig. 12-14. Figs. 12-14 clearly show that the maximum energy absorbed is for mode C and minimum is for mode A for all the three representative days. It is quite interesting to see that the energy absorbed by the base plate on Dec-21 for mode C is 118% more than the corresponding value for mode A, while the energy absorbed by the walls is almost the same and the total energy absorbed for mode C is 89% higher than the energy absorbed by the mode A. On Jun-21 for mode C the energy absorbed over the day by the base plate, walls and total energy is 18 times, 5.3 times and 14 times more than the corresponding values for tracking mode A. Another interesting point to observe is that the total energy absorbed over a day for non-tracked mode (A) on Dec-21(840 kJ) is 10 times more than the energy absorbed on Jun-21 (80 kJ). On comparing the tracking modes B and C it has been found that the percent difference in the total energy absorbed for the two modes is 1.5%, 32% and 177% for Dec-21, Mar-21 and Jun-21, respectively.

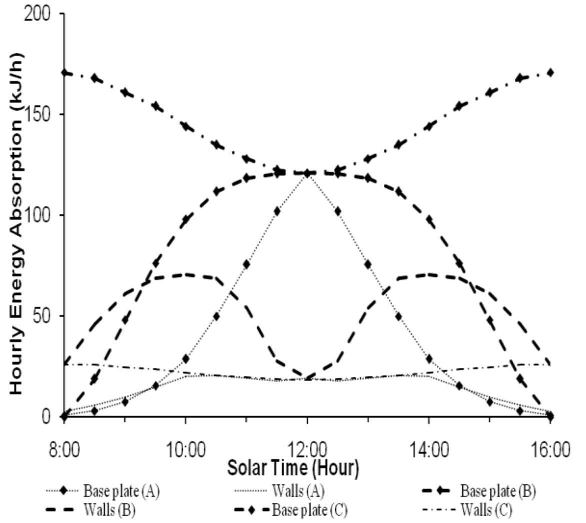

Fig. 13. Variation in hourly energy absorbed by the base plate and walls of the solar collector for different tracking modes A, B and C for reflected radiation on Mar-21 ($\delta=0^o$).

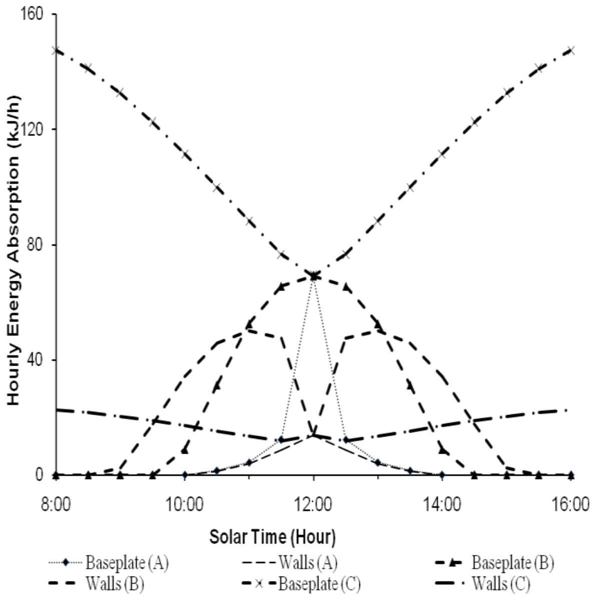

Fig. 14. Variation in hourly energy absorbed by the base plate and walls of the solar collector for different tracking modes A, B and C for reflected radiation on Jun-21 ($\delta = 23.45^o$).

The formalism can prove to be useful in better designing of flat plate collector- reflector systems and in improving performance.

6. Conclusions

A mathematical formalism has been developed for estimating energy absorbed by the base plate and walls of the absorber tray of a flat plate collector for reflected radiation. Expressions for useful reflected radiation receiving areas for base plate and walls of absorber tray for various cases such as non-tracked, azimuthally tracked collector but mirror angle not adjusted and fully tracked modes have been developed and presented. Results of calculations for hot box solar cooker CSC have been reported. The study shows that the maximum reflected energy is absorbed on Dec-21 followed by Mar-21 and Jun-21. If reflector angle is kept fixed the energy absorption in summers is for very short duration and only 10-12% of the solar radiation is absorbed. The study reveals that the radiation absorbed by the base plate in December is 18% more for the systems with inclined walls though the energy absorbed by the walls is almost equal whereas the energy absorption by the base plate and walls is 10-40% higher in March and June for the system with inclined walls. This indicates that more effective heating of load can be achieved for collectors with inclined walls. The study of various tracking modes shows that for December the azimuthally tracked and fully tracked modes are almost equivalent. Tracking requirements are more in summers and the energy absorption for fully tracked mode is 177% higher than the non tracked mode.

This formalism can be used in general for any flat plate collector-reflector systems to study the energy distribution pattern on walls and base plate of a four walled absorber tray for reflected radiation. It can also be used to study solar hot boxes with inclined walls, different walls and base plate materials, and aid in efficient designing.

References

[1] S. H. Zakaria, A. Khaled, H. Mustapha, "Experimental study of flat plate solar collector equipped with concentrators", International Journal of Renewable Energy Research, Vol. 7, No.3, 1028-1031, 2017. (Article)

[2] K.Uchida, T. Senjyu, A.Yona, U.Naomitsu, "Optimum design of PV and SWH for all-electric house" International Conference on Renewable Energy Research and Applications Nagasaki, 11-14 Nov. 2012 (Conference paper).

[3] R. Bayindir, E. Kabalci, H. I. Bulbul, C. Can, "Optimization of operating conditions of photovoltaic systems: A case study", International Conference on Renewable Energy Research and Applications, Nagasaki, 11-14 Nov. 2012 (Conference paper).

[4] E.U. Khan, A.R. Martin, "Hybrid renewable energy with membrane distillation polygeneration for rural households in Bangladesh: Pani Para Village case study" _International Conference on Renewable Energy Research and Application, Milwaukee, 19-22 Oct. 2014 (Conference paper).

[5] Y. Yoshida, Y. Ueda, "Verification of consumer's benefits for different area ratio of PV array and solar thermal water heater considering regional characteristics", 2015 International Conference on Renewable Energy Research and Applications, Palermo, 22-25 Nov. 2015 (Conference paper).

[6] V. Msomi, O. Nemraoui, "Improvement of the performance of solar water heater based on nanotechnology", 6th International Conference on Renewable Energy Research and Applications, San Diego, 5-8 Nov. 2017 (Conference paper).

[7] S. C. Seitel, "Collector performance enhancement with flat reflectors", Solar Energy, Elsevier, Vol. 17, pp. 291-295, 1975. (Article)

[8] S.L. Grassie and N.R.Sheridan "The use of planar reflectors for increasing the energy yield of flat-plate collectors", Solar Energy, Elsevier, Vol.19, pp. 663-668, 1977. (Article)

[9] N. E.Wijeysundera, "Geometric factors for plane specular reflectors", Solar Energy, Elsevier, Vol. 20, pp. 81-85, 1978. (Article)

[10] D. P.Grimmer, K.G. Zinn, K.C. Herr and B.E. Wood, "Augmented solar energy collection using different types of planar reflective surfaces; theoretical calculations and experimental results", Solar Energy, Elsevier, Vol. 21, pp. 497-501, 1978. (Article)

[11] I. S. Taha and S. M. Eldighidy, "Effect of off-south orientation on optimum conditions for maximum solar energy absorbed by flat plate collector augmented by plane reflector", Solar Energy, Elsevier, Vol. 25, pp. 373-379, 1980. (Article)

[12] D. C. Larson, "Optimization of flat-plate collector-flat mirror systems", Solar Energy, Vol. 24, pp. 203-7, 1980. (Article)

[13] H.F. Chiam, "Stationary reflector-augmented flat-plate collector", Solar Energy, Elsevier, Vol. 29, pp. 65-69, 1982. (Article)

[14] A. Dang, "Collector, collector-reflector systems-an analytical and practical study", Energy Conversion & Management, Elsevier, Vol. 26, pp. 33-39, 1986. (Article)

[15] H.P. Garg and D.S.Hrishikesan, "Enhancement of solar energy on flat-plate collector by plane booster mirrors", Solar Energy, Elsevier, Vol. 40, pp. 295-307, 1988. (Article)

[16] A.V.N. Rao, T. L. S. Rao and S. Subramanyam, "Mirror boosters for solar cookers-III", Energy Conversion & Management, Elsevier, Vol. 32, pp. 51-58, 1991. (Article)

[17] H.M.S. Hussein, G. E. Ahmad and M. A. Mohamad, 'Optimization of operational and design parameters of planar reflector-tilted flat plate solar collector systems', Energy, Elsevier,Vol. 25, pp. 529-42, 2000. (Article)

[18] H. Tanaka, "Solar thermal collector augmented by flat plate booster reflector: Optimum inclination of collector and reflector", Applied Energy, Elsevier,Vol. 88, pp.1395-1404, 2011. (Article)

[19] B. Matthew, "Analytical model for solar irradiance near a planar vertical diffuse reflector-Formulation, validation and simulations", Solar Energy, Elsevier, Vol. 91, pp. 79-92, 2013. (Article)

[20] N. Nikolic and N. Lukic, "Theoretical and experimental investigation of the thermal performance of a double exposure flat-plate solar collector", Solar Energy, Elsevier, Vol. 119, pp. 100-113, 2015. (Article)

[21] Z. T. Pavlovic and LjT. Kostic, "Variation of reflected radiation from all reflectors of a flat plate solar collector during a year", Energy, Elsevier, Vol. 80, pp. 75-84, 2015. (Article)

[22] G. Coccia, G. Di Nicola, M. Pierantozzi, S. Tomassetti, A. Aquilanti, "Design, manufacturing, and test of a high concentration ratio solar box cooker with multiple reflectors", Solar Energy, Elsevier, Vol. 155, pp. 781–792, 2017. (Article)

[23] Z. Guidaraa, M. Souissia, A. Morgenstern, A. Maalej, "Thermal performance of a solar box cooker with outer reflectors: Numerical study and experimental investigation", Solar Energy, Elsevier, Vol.158, pp. 347–359, 2017. (Article)

[24] A. A. Sagade, S.K. Samdarshi, P.S. Panja, "Experimental determination of effective concentration ratio for solar box cookers using thermal tests", Solar Energy, Elsevier, Vol. 159, pp. 984–991, 2018. (Brief note)

[25] N. M. Nahar and H. P. Garg, "Free convection and shading due to gap spacing between an absorber plate and the cover glazing in solar energy flat-plate collectors", Applied Energy, Elsevier, Vol. 7, pp. 129-145, 1980. (Article)

[26] N. Sengar, P. Dashora, S. Mahavar and R. C. Punia, "Mathematical formalism to study energy distribution pattern in solar hot boxes for global solar radiation", International Journal of Innovative Research in Science, Engineering and Technology, Vol. 3 No.12, pp.18147-56, 2014. (Article)

[27] N. Sengar, P. Dashora and S. Mahavar, "Low cost solar cooker: Promising solution towards reducing indoor air pollution from solid fuel use" Indian Journal of Science and Technology, iSEE, Vol. 3 No. 10, pp. 1038-1042, 2010. (Article)

[28] S. Mahavar, N. Sengar, P. Rajawat, M. Verma and P. Dashora, "Design development and performance studies of a novel single family solar cooker", Renewable Energy, Elsevier, Vol. 47, pp. 67-76, 2012. (Article)

[29] J.A. Duffie and W.A. Beckman, Solar Engineering of Thermal Processes, John Wiley & Sons, New Jersey, 2006. (Book)

[30] S. P. Sukhatme, Solar Energy: Principles of Thermal Collection and Storage, Tata McGraw Hill, New Delhi, 1996. (Book)

[31] J. F. Kreider and F. Kreith, Solar Energy Handbook, McGraw Hill, New York, 1981. (Book)